

This Page Is Inserted by IFW Operations  
and is not a part of the Official Record

## **BEST AVAILABLE IMAGES**

Defective images within this document are accurate representations of the original documents submitted by the applicant.

Defects in the images may include (but are not limited to):

- BLACK BORDERS
- TEXT CUT OFF AT TOP, BOTTOM OR SIDES
- FADED TEXT
- ILLEGIBLE TEXT
- SKEWED/SLANTED IMAGES
- COLORED PHOTOS
- BLACK OR VERY BLACK AND WHITE DARK PHOTOS
- GRAY SCALE DOCUMENTS

**IMAGES ARE BEST AVAILABLE COPY.**

**As rescanning documents *will not* correct images,  
please do not report the images to the  
Image Problem Mailbox.**

0002  
attach #9



IN THE UNITED STATES PATENT AND TRADEMARK OFFICE

RECEIVED  
JUL 08 2003  
TC 1700

In re Application of:

Saban et al.

: Group Art Unit: 1744

Serial No.: 08/963,678

: Examiner: McNeil, J.

Filed: October 31, 1997

For: MICROBAND ELECTRODE ARRAYS

Certificate of Mailing  
I hereby certify that this  
correspondence is being deposited  
with the United States Postal  
Service with sufficient postage as  
First Class Mail in an envelope  
addressed to: Assistant Commissioner  
for Patents, Washington, D.C. 20231

6/24/99 *Lee Blevans*  
Date of Mailing LBA BLEVANS

DECLARATION OF STEVEN B. SABAN

Asst. Commissioner for Patents  
Washington, D.C. 20231

Sir:

I Steven B. Saban declare that:

I am a coinventor of the above-referenced patent application;

I measured the cyclic voltammogram presented as exhibit A using a linear 24-Au-electrode microband array in which the thickness of each electrode was 0.18 micrometers, the width of each electrode was 10 micrometers and the spacing between electrodes was 400 micrometers. The voltammogram was measured in 50 mM  $K_3[Fe(CN)_6]$  with a 1 M KCl supporting electrolyte. The forward and reverse scans of the cyclic voltammogram at a scan rate of 200 mV/sec overlap indicating that a steady-state has been achieved;

I also measured the cyclic voltammograms presented in Fig. 11 of the specification of the above-referenced application ( in 5 mM  $K_3[Fe(CN)_6]$  with a 1 M KCl supporting electrolyte). The graph illustrated with the heavier line is the cyclic voltammogram of a linear 24-Au-electrode microband array. The graph shows a small deviation of the forward and reverse scans. As described in the specification at page 28 (bottom of the page) the array of twenty-four Au electrodes at that time the graph of Fig. 11 was measured exhibited an unusually high limiting current believed due to a less than ideal seal. Further, the graph of Fig. 10 (experiment) measured using the same 24-Au-electrode array shows a deviation due to a large capacitive discharge typically observed if the electrode seal leaks. The same 24-Au-electrode microband array was used to measure the cyclic voltammograms of both Fig. 11 (heavy line) and exhibit A except that the surface of the array had been repolished before Fig.11 was obtained. Repolishing corrected the seal leakage in the electrode;

In addition, I measured the chronoamperometric graph of Fig. 9 using the 24-Au-electrode array described above, before repolishing (see page 28 lines 14-16). The graph shows steady-state behavior because the current vs. time graph reaches a horizontal asymptote within about 2 seconds. The current does not substantially change with time after equilibrium is reached (about 2 seconds). The electrodes of our invention exhibit true steady-state behavior;

I have reviewed Thormann et al. (1984) Anal. Chem. 57: 2764 -2770. The cyclic voltammograms in Fig.3 and Fig. 4 of that paper do not exhibit steady-state behavior, since the forward and reverse scans of the voltammogram do not overlap at slow scan rates. The reference Bond et al. (1986) J. Phys. Chem. 90: 2911-2917, which has two coauthors in common with Thormann et al. discusses steady-state voltammograms on pages 2914 and 2915. The authors indicate that a steady-state response shows "complete overlap of forward and reverse scans" and is governed by equation 10 (bottom of page 2914). Nonsteady-state response is not governed by equation 10 and "a separation between forward and reverse sweeps is apparent." The cyclic voltammograms of Fig. 3 of Bond et al. show separation of forward and reverse sweeps and illustrate non-steady-state response. The cyclic voltammograms of Thormann et al. in Figs. 3

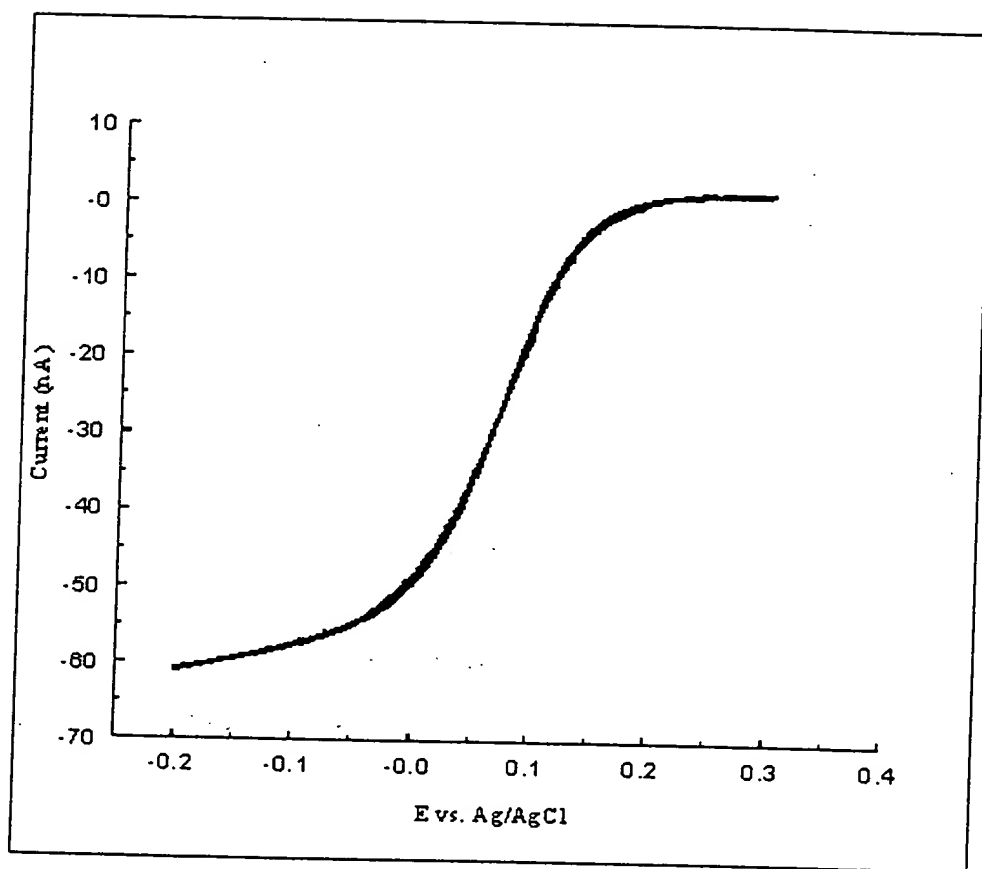
and 4 exhibit separations in the forward and reverse sweeps that are similar to those associated in Bond et al. with a nonsteady-state response;

I further declare that all statements made herein of my own knowledge are true and that all statements made on information and belief are believed to be true; and further that these statements were made with the knowledge that willful false statements and the like so made are punishable by fine or imprisonment, or both, under Section 1001 of Title 18 of the United States Code, and that such willful false statements may jeopardize the validity of the above-referenced application or any patent issuing thereon.

6/21/99  
DATE

  
STEVEN B. SABAN

EXHIBIT A



Steady-state cyclic voltammogram for an array of 24 Au microband electrodes in 50 mM  $\text{K}_3[\text{Fe}(\text{CN})_6]$  with a 1 M KCl supporting electrolyte. Scan rate = 200 mV/s

# Theory and Experimental Characterization of Linear Gold Microelectrodes with Submicrometer Thickness

Alan M. Bond,\* Terry L. E. Henderson, and Wolfgang Thormann<sup>1</sup>

Division of Chemical and Physical Sciences, Deakin University, Waurn Ponds, Victoria, 3217, Australia  
(Received: August 12, 1985; In Final Form: December 26, 1985)

The theory of cyclic voltammetry at linear gold microelectrodes of thicknesses less than 1  $\mu\text{m}$  has been examined for electrode processes where the electron-transfer step is rate determining. Digital simulation (expanding-grid method) is used with cylindrical processes where the electron-transfer step is rate determining. Results of the theory in the limit of the reversible response are in agreement with diffusion in all theoretical calculations. Results of the theory in the limit of the reversible response are in agreement with previously published theories and with experimental data obtained in this work. Unlike microdisk electrodes, departures from the steady-state sigmoidal shaped curves are expected and observed experimentally, provided considerable attention is given to electrode design. The very thin electrodes achieve the desirable goal of having almost purely cylindrical diffusion and consequently may be used in high-resistance solutions and for measurements of very fast rates of electron transfer. The large total area, provided by the dimension of length, means that measured currents can be sufficiently large so that transient voltammetric methods may be implemented with conventional instrumentation. The combined use of computer modeling of the theory and comparison of experimental data obtained from microdisk electrodes, linear arrays of microdisk electrodes, linear microelectrodes, and microring electrodes has enabled microelectrodes to be systematically classified. The linear electrodes with submicrometer width are a subset of microelectrodes ranging from the two extremes, the microdisk and the microring electrodes.

## Introduction

Microelectrodes have become an important development in electrochemistry in the last decade. Microdisk electrodes have been predominantly used for fundamental studies,<sup>2-6</sup> microcylinder electrodes have been applied widely to biological measurements,<sup>6</sup> single fibre microelectrodes have been used for capillary LC/EC detection,<sup>7</sup> and arrays of microdisk electrodes have been employed as analytical sensors in flow through cells.<sup>8,9</sup> More recently, Wightman et al.<sup>10</sup> described fabrication methods for microcylinder, band, and tubular band electrodes. The majority of these studies are characterized by electrodes having radii or thicknesses greater than 1  $\mu\text{m}$ . More recently some emphasis has been placed on considerably smaller electrodes. For instance, a 0.3- $\mu\text{m}$  radius platinum microdisk electrode has been constructed,<sup>11</sup> ring microelectrodes with a thickness of 0.05–0.4  $\mu\text{m}$  have been reported,<sup>12</sup> linear arrays of microdisk electrodes have been fabricated from 0.1- $\mu\text{m}$  thin gold layers,<sup>13</sup> and the electroanalytical properties of band electrodes of submicrometer width have been described.<sup>14</sup> A final interesting example given is the formation of extremely small mercury electrodes attached to carbon substrates.<sup>15</sup>

Electrodes of very small thicknesses or radii may exhibit very little linear diffusion and have unique characteristics enabling them to be used in high-resistance media<sup>11</sup> and short time domains.<sup>16,17</sup> The response for electrode processes where the electron transfer is rate determining has been examined theoretically by computer simulation at a microdisk electrode<sup>18</sup> and for ensembles of microelectrodes<sup>19</sup> while analytical expressions derived for microdisk electrodes<sup>20</sup> and for microcylinder electrodes<sup>21</sup> have allowed numerical calculations of theoretical voltammograms for reversible electrode processes in these cases.

In this paper, work on line electrodes has been extended in several important areas from that described by Wightman and colleagues<sup>10,14</sup> and others.<sup>22-24</sup> Wightman et al.<sup>14</sup> have already indicated that such electrodes should be useful for studying fast rates of electron transfer, although as noted in their paper, no theoretical description of the appropriate mechanism is available for this purpose. In our work, a theoretical description of such an electrode process is presented and applied to oxidation of ferrocene in acetonitrile. Furthermore, the theoretical prediction of a non-steady-state current at negative potentials, not observed in ref 14, is considered, as is the use of transient electrochemical methods made possible by the large total area of the electrode and the use of such electrodes in high-resistance media (no deliberately added electrolyte).

Finally, the question of possible advantages over microdisk and array microelectrodes is considered. Very thin linear microelectrodes are attractive compared with ring microelectrodes, microcylinder electrodes, or microdisk electrodes of equivalent dimensions because of the simplicity of fabrication. The wide availability of extremely flat glass plates (e.g., microscope slides) also means that they are inherently inexpensive to manufacture

(1) Present address: Center for Separation Science, University of Arizona, ECE Bldg. 20, Tucson, AZ 85721.

(2) Bindra, P.; Brown, A. P.; Fleischmann, M.; Pletcher, D. *J. Electroanal. Chem.* 1975, 58, 31.

(3) Dayton, M. A.; Brown, J. C.; Stuts, K. J.; Wightman, R. M. *Anal. Chem.* 1980, 52, 946.

(4) Dayton, M. A.; Ewing, A. G.; Wightman, R. M. *Anal. Chem.* 1980, 52, 2392.

(5) Fleischmann, M.; Lasserre, F.; Robinson, J.; Swan, D. *J. Electroanal. Chem.* 1984, 177, 97.

(6) Wightman, R. M. *Anal. Chem.* 1981, 53, 1125A.

(7) Knecht, L. A.; Guthrie, E. J.; Jorgenson, J. W. *Anal. Chem.* 1984, 56, 479.

(8) Caudill, W. L.; Howell, J. O.; Wightman, R. M. *Anal. Chem.* 1982, 54, 2532.

(9) Sleszynski, N.; Osteryoung, J.; Carter, M. *Anal. Chem.* 1984, 56, 130.

(10) Kovak, P. M.; Caudill, W. L.; Peters, D. G.; Wightman, R. M. *J. Electroanal. Chem.* 1985, 185, 285.

(11) Bond, A. M.; Fleischmann, M.; Robinson, J. *J. Electroanal. Chem.* 1984, 163, 299.

(12) MacFarlane, D. R.; Wong, D. K. Y. *J. Electroanal. Chem.* 1985, 185, 197.

(13) Thormann, W.; van den Bosch, P.; Bond, A. M. *Anal. Chem.* 1985, 57, 2764.

(14) Wehmeyer, K. R.; Deakin, M. R.; Wightman, R. M. *Anal. Chem.* 1985, 57, 1913.

(15) Scharifker, B.; Hills, G. *J. Electroanal. Chem.* 1981, 130, 31.

(16) Hepel, T.; Osteryoung, J. *J. Phys. Chem.* 1982, 86, 1406.

(17) Howell, J. O.; Wightman, R. M. *J. Phys. Chem.* 1984, 88, 3915.

(18) Heinze, J. *Ber. Bunsenges. Phys. Chem.* 1981, 85, 1096.

(19) Reller, H.; Kirowa-Eisner, E.; Gileadi, E. *J. Electroanal. Chem.* 1984, 161, 247.

(20) Aoki, K.; Akimoto, K.; Tokuda, K.; Matsuda, H.; Osteryoung, J. *J. Electroanal. Chem.* 1984, 171, 219.

(21) Aoki, K.; Honda, K.; Tokuda, K.; Matsuda, H. *J. Electroanal. Chem.* 1985, 182, 267.

(22) Kittlesen, G. P.; White, H. S.; Wrighton, M. S. *J. Am. Chem. Soc.* 1984, 106, 7339.

(23) Saito, Y. *Rev. Polarogr.* 1963, 11, 177.

(24) Symanski, J. S.; Bruckenstein, S. *J. Electrochem. Soc.* 1984, 131, 110C.

in high quality<sup>14</sup> which is a practical advantage. However, to develop ideas on microelectrodes further, the relationship between microdisk electrodes, linear arrays of microdisk electrodes, linear microelectrodes, and ring microelectrodes is examined to identify the similarities so that predictions on the attributes of the different classes of microelectrodes may be realistically undertaken.

### Experimental Section

(a) *Instrumentation.* (i) *Three-Electrode Format.* Conventional potentiostatic three-electrode assemblies were employed for currents larger than 50 nA. A BAS 100 electrochemical analyzer (Bioanalytical Systems, West Lafayette) interfaced into a Houston Instrument HILOT DMP-40 plotter was used as the function generator and data acquisition and recording system in a regular three-electrode mode or by connecting both the reference and the auxiliary leads to the reference electrode in a two-electrode arrangement. A Metrohm E611 VA detector was also employed together with the wave generator and the data acquisition provided by the Motorola D2 "Kit".<sup>25</sup> This configuration permits data to be transferred to a Sphere 6809 microprocessor system (Paris Electronics, Sydney) and subsequently to a DEC 20/60 computer if required,<sup>26</sup> thereby enabling data storage, data evaluation, and background correction to be made.

(ii) *Two-Electrode Format.* The following instrumental configurations in the two-electrode format were used to measure the small currents provided by single microdisk electrodes. A Metrohm VA-Scanner Model E612 was employed as the function generator, a Keithley 480 picoammeter as the current measuring device, and a Houston Instruments Omnigraphic 2000 XY recorder for the data plots. Function generation and data acquisition were performed in another approach by employing the Motorola D2 "Kit" together with the Keithley electrometer as the ammeter.

(iii) *Electrodes.* Single gold microdisk electrodes were constructed at the University of Southampton similar to the platinum microelectrodes reported in ref 11. They consist of 2.5–30- $\mu$ m-radius metal wires sealed into glass. Conventional circular disk electrodes (BAS) with 0.8 mm radius and embedded in a plastic rod of 6.5 mm diameter as well as linear inlaid microelectrode arrays<sup>13</sup> were also used as working electrodes for comparison purposes. The construction of the straight line microelectrodes is discussed in a separate section. A Ag/Ag<sup>+</sup> (0.1 M AgNO<sub>3</sub>) double fritted system in acetonitrile was used as the reference electrode. A platinum wire served as a counter electrode in the three electrode assemblies referred to above. All experiments were performed in a solid aluminum Faraday cage. Electrodes were polished in accordance with established procedures.<sup>11</sup>

(b) *Electrode Fabrication.* Methods for construction of line electrodes were extensions of those developed by Wightman et al.<sup>14</sup> However, care must be taken in the construction to obtain the theoretically predicted shape (see later). (i) *Techniques.* The construction of straight line gold microelectrodes was investigated by producing thin films with metalloorganics and vapor deposition of gold onto glass or polyester. Formulated metalloorganics, supplied by Engelhard Corp., East Newark, NJ, provide a means of obtaining thin metal films on ceramics or glass. The manufactured "inks" contain up to 25% noble metal, are metallic solutions with no discrete particles in suspension, and include glass-forming base components. The major fraction consists of organics which must be thermally decomposed. The incorporated base metals oxidize during the heat treatment to form an oxide layer necessary for the bonding between the metal film and the substrate. Depending upon the amount of noble metal, film thicknesses from 0.05 to 0.2  $\mu$ m are thereby obtained. Metalloorganics applied on glass plates by silk screening were previously used for the design of linear inlaid microelectrode arrays.<sup>13</sup>

Vapor deposition or sputtering of gold onto glass are routinely utilized in many areas of microelectronics and microinstrumentation.

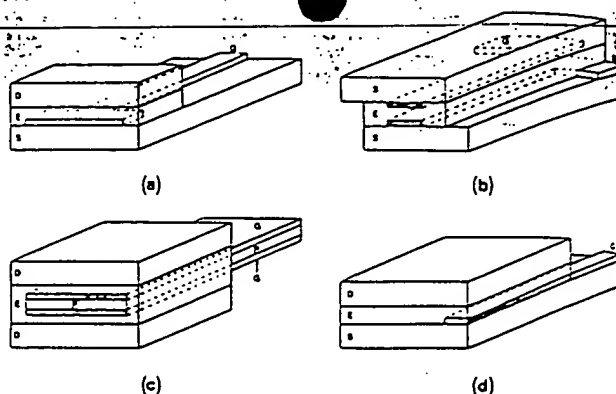


Figure 1. Construction principles of linear microelectrodes for voltammetry. Fabrication with metallized glass plates (a, b, d) and metallized plastic sheets (c). S = glass substrate; D = cover glass plate; E = epoxy resin; G = connecting side; P = plastic sheet.

tation.<sup>27</sup> A 50–70- $\text{\AA}$  chromium layer is commonly first coated onto the glass surface for the improvement of the bond between the gold and the substrate. Gold layers of 100–10 000  $\text{\AA}$  are thereby readily produced. This method was used for the fabrication of linear microelectrode arrays<sup>13</sup> and for the construction of ring microelectrodes.<sup>12</sup> The direct vapor deposition of gold onto polyester represents an interesting alternative.<sup>28,29</sup> It provides the opportunity for simple fabrication of multiple parallel line microelectrodes as reported in this work. The realization of a "spiral" or "snail" electrode, and other related geometries (see Figure 6), should also be possible. Other applications of such metallized plastic films range from optically transparent electrodes<sup>23,29</sup> to potential gradient microsensors in capillary electrophoresis (two parallel microrings with the diameter of the capillary<sup>30</sup>). The Mylar sheets (Melinex polyester films, ICI Plastics Division, Welwyn Garden City, UK) used in this work were gold coated at the University of Bern, Switzerland, with a Balzers apparatus. A similar product is commercially available from Sierracin/Sylmar (Sylmar, CA) under the trade name Intrex-G.<sup>29</sup>

The lengths investigated cover the range from 5 to 60 mm and the thickness varied from 0.1 to 0.9  $\mu$ m. The spacing between parallel lines was 20–50  $\mu$ m. The various fabrication procedures shall be discussed in turn.

(ii) *Fabrication of Straight Line Electrodes with Metalloorganics.* The construction of straight line electrodes with metalloorganics is depicted in Figure 1a. A T shape pattern of metalloorganics was applied onto a conventional microscope slide with a Pasteur pipet containing a small amount of the gold solution. The ink was dried in a stream of warm air (hair dryer) prior to a 20-min air firing at 680  $^{\circ}\text{C}$ .<sup>13</sup> A second but smaller microscope slide was glued on top of the gold-bearing plate with an epoxy resin (Super Strength Araldite, Ciba-Geigy Australia Ltd). The cover plate is pressed on during the 24-h curing period of the resin, resulting in a very thin epoxy layer of 10–15  $\mu$ m. Polishing of the front side occurred as described below. The connecting part of the T shape gold layer was contacted with a modified alligator clip having a silver alloy tip soldered to the top part (which is the conducting side) and a plastic embedded lower part. An electrode consisting of two parallel lines was also constructed by using a gold-bearing cover plate. The fabrication principle is depicted in Figure 1b and allows individual access to the two microlines.

(iii) *Fabrication of Straight Line Gold Electrodes from Metallized Plastic Films.* A narrow strip of the gold-coated Mylar was carefully glued between two microscope slides using Araldite as depicted in Figure 1c. After a curing period of at least 24 h

polishing of the front side protruded the same length, permitting simple connection and an alligator clip. (iv) *Fabrication of Posited Thin Gold Electrodes.* Thin strips of gold were deposited on the side of the part of a microscope slide the narrow gold strip occurred as described. Connection with the modified alligator clip of the assembly to var electrode lengths.

(v) *Polishing of the assembly.* Polishing was first then polished by hand working down in the polishing with aluminum commercial metal polish. It is important to note that two glass plates in the assembly. The polishing range of 5–15  $\mu$ m

### Theory

Linear electrode of constricted mass is purpose of the theory be considered as has been suggested is based on that for the microcylinder from the actual reaction

where both components containing a large excess cylinder electrode

where  $C_j$  is the concentration from the axis of the species,  $r$  is the radius exchanged per species. Initial concentration  $R$  in which  $C_R =$  surface,  $r = a$ , then

$$I = n$$

In case of a rapid considered as full yields

$$(Co)_{\infty}$$

where  $E$  is the electrode at which no electrode at a rate  $v$  in the electrochemical reaction. It was decided was previously electrodes but no procedure referred inclusion of elec

(27) Wohltjen, H. *Anal. Chem.* 1984, 56, 87A.

(28) Winograd, N.; In *Laboratory Techniques in Electroanalytical Chemistry*; Kissinger, P. T., Heinemann, W. R., Eds.; Marcel Dekker: New York, 1984; p 321.

(29) Cieslinski, R.; Armstrong, N. R. *Anal. Chem.* 1979, 51, 565.

(30) Thormann, W. PhD Dissertation, University of Bern, Switzerland, 1981.

(25) Anderson, J. E.; Bagchi, R. N.; Bond, A. M.; Greenhill, H. B.; Henderson, T. L. E.; Walter, F. L. *Am. Lab. (Fairfield, Conn.)* 1981, 13 (February), 21.

(26) Bond, A. M.; Greenhill, H. B.; Heritage, I. D.; Reust, J. B. *Anal. Chim. Acta* 1984, 165, 209.

polishing of the front side occurred as described below. The strip protruded the sandwiched assembly about 1 cm on one side permitting simple connection with a piece of conductive silicone and an alligator clip.

(iv) *Fabrication of Straight Line Electrodes from Vapor Deposited Thin Gold Films on Glass.* Small glass plates bearing thin strips of gold (about  $30 \times 0.5$  mm) were cut from the connecting side of the three-element gold arrays described in ref 13. Part of a microscope slide was cemented with Araldite on top of the narrow gold strip (Figure 1d). Polishing of the front side occurred as described below after the epoxy resin was completely cured. Connection was achieved on the top end of the gold strip with the modified alligator clip referred to above. Immersion of the assembly to various depths permits the investigation of different electrode lengths.

(v) *Polishing of Linear Microelectrodes.* The front side of each assembly was first ground flush on a rotating diamond disk, and then polished by hand on wet sandpaper, starting with B500 and working down in steps to P1200. This was followed by further polishing with alumina ( $1 \mu\text{m}$ ) water slurries and ordinary commercial metal polish (Brasso, household quality) on paper. It is important to note that a thin, insulating epoxy layer between the two glass plates is required for the proper performance of the assembly. The polymer (epoxy) thickness was found to be in the range of  $5\text{--}15 \mu\text{m}$  by using a scanning electron microscope.

### Theory

Linear electrodes as constructed in this work (Figure 1) have restricted mass transport (diffusion) to the electrode. For the purpose of the theory used in this investigation the electrodes will be considered as half cylinders with very small radii. This model has been suggested by Wightman et al.<sup>10,14</sup> The actual theory is based on that for stationary microcylinder electrodes in which the microcylinders have the equivalent surface area calculated from the actual linear electrodes used. For a simple electrode reaction



where both components R and O are soluble in a solution containing a large excess of supporting electrolyte, and for a stationary cylinder electrode the diffusion equation yields

$$\frac{\partial C_j}{\partial t} = D \left( \frac{1}{r} \right) \frac{\partial}{\partial r} \left[ r \left( \frac{\partial C_j}{\partial r} \right) \right] \quad (2)$$

where  $C_j$  is the concentration of species R or O,  $r$  is the distance from the axis of the electrode,  $D$  is the diffusion coefficient of both species,  $t$  is the electrolysis time,  $n$  is the number of electrons exchanged per species R, and  $k_j$  is the charge-transfer rate constant. Initial conditions are given by a solution with component R in which  $C_R = C_R^*$  and  $C_O = 0$  at  $t = 0$ . At the electrode surface,  $r = a$ , the current density  $I$  is expressed by

$$I = nFD \left( \frac{\partial C_R}{\partial r} \right)_{r=a} = -nFD \left( \frac{\partial C_O}{\partial r} \right)_{r=a} \quad (3)$$

In case of a rapid electrode reaction in which the system can be considered as fully reversible (Nernstian conditions) the relation holds

$$(C_O)_{r=a}/(C_R)_{r=a} = \exp[nF(E - E^0)/RT] \quad (4)$$

where  $E$  is the electrode potential which is initially held at a value at which no electrode reaction takes place and is swept linearly at a rate  $v$  in the negative direction. Other symbols have the usual electrochemical meaning. These equations can be solved by numerical calculations as described by Aoki et al.<sup>21</sup>

It was decided to employ the method of digital simulation which was previously applied to single<sup>18</sup> and arrays<sup>19</sup> of microdisk electrodes but not to microcylinders. In contrast to the numerical procedure referred to above<sup>21</sup> computer modeling permits simple inclusion of electrode kinetics for the heterogeneous electron-

TABLE I: Comparison of Data Obtained by Computer Simulation and by Approximating Analytical Solution (Eq 8) for Reversible One-Electron Oxidation in Presence of Large Excess of Supporting Electrolyte<sup>a</sup>

width of linear electrode, $\mu\text{m}$	corros microcylinder rad, $\mu\text{m}$	peak current	
		from simuln, $\mu\text{A}$	calcd from eq 8, $\mu\text{A}$
0.2	0.0318	1.85	1.94
2.0	0.318	2.77	2.79
20.0	3.183	4.60	4.54
100.0	15.915	8.36	8.31

<sup>a</sup> Assumed conditions: initial concentration of R, 1 mM; electrode length = 1.18 cm;  $D = 2.3 \times 10^{-5} \text{ cm}^2/\text{s}$ ; sweep rate,  $v = 50 \text{ mV/s}$ ;  $k^0 = 10000 \text{ cm/s}$ ;  $\alpha = 0.5$ ;  $E^0 = 37 \text{ mV}$ ; initial potential =  $-200 \text{ mV}$ ; final potential =  $300 \text{ mV}$ ; step size =  $0.0001 \text{ mV}$  for electrode width  $\leq 2 \mu\text{m}$  and  $0.001$  for  $> 2 \mu\text{m}$ .

transfer process, so that the prediction of both the reversible and the quasi-reversible system is readily available. The treatment used here is based upon the Butler-Volmer model expressed by the reaction rates<sup>31</sup>

$$R_f = k_f(C_R)_{r=a} = k^0(C_R)_{r=a} \exp[\alpha nF(E - E^0)/RT] \quad (5)$$

$$R_b = k_b(C_O)_{r=a} = k^0(C_O)_{r=a} \exp[-(1 - \alpha)nF(E - E^0)/RT] \quad (6)$$

where  $k^0$  is the heterogeneous charge-transfer rate constant and  $\alpha$  is the charge-transfer coefficient, usually regarded as potential-independent. For very large values of  $k^0$  ( $> 100 \text{ cm/s}$ ) the model describes a reversible (Nernstian) one-electron oxidation with a deviation  $< 1\%$ . The complete current-potential equation is given by

$$I = F(R_f - R_b) \quad (7)$$

The simulation program used in this work was based on the optimized explicit finite difference method<sup>32</sup> with appropriate modifications for cylindrical geometry. An exponential expanding grid was employed. The grid size was reduced until consistent values independent of grid size were obtained. The implementation of the program occurred on a DEC 20/60 computer. The contributions of the areas from the top and the bottom of the microcylinder to the total area of the microcylinder were neglected and for a given radius the model assumed a linear relationship between electrode length and current. To check the accuracy of the simulation data, peak currents for a range of cylinder radii and for a reversible one-electron oxidation were calculated by using the appropriate expression for peak current density<sup>21</sup>

$$I_p a / nFC_R^* D = 0.446p + 0.335p^{0.15} \quad (8)$$

where  $p = (nFa^2v/RTD)^{1/2}$ . Table I shows that excellent agreement was obtained.

### Results and Discussion

The electrode process chosen as a model for theoretical and experimental comparisons is the one-electron oxidation of ferrocene (fc) to the ferrocenium cation (fc<sup>+</sup>)



in acetonitrile. The rate of electron transfer for this electrode process in acetonitrile at conventional platinum electrodes ( $0.1 \text{ M TBAP}$ ,  $22^\circ \text{C}$ ) is  $0.09 \text{ cm/s}$ .<sup>33</sup> Under these experimental conditions this can be assumed to be close to a diffusion-controlled reversible process. Furthermore the diffusion coefficient is known to be  $2.3 \times 10^{-5} \text{ cm}^2/\text{s}$ .<sup>11</sup>  $E^0$  was taken as  $E_{1/2}$  value of the

(31) Bond, A. M. *Modern Polarographic Methods in Analytical Chemistry*; Marcel Dekker: New York, 1980.

(32) Feldberg, S. W. *J. Electroanal. Chem.* 1981, 127, 1.

(33) Kadish, K. M.; Ding, J. Q.; Malinski, T. *Anal. Chem.* 1984, 56, 1741.

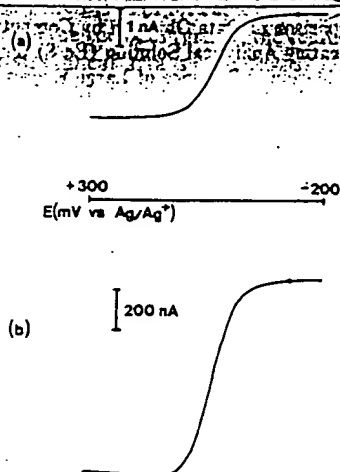


Figure 2. Linear sweep voltammograms at 2.5- $\mu$ m-radius gold microelectrode (a) and at a linear gold microelectrode of 1.18 cm length and about 0.6  $\mu$ m width (b) for oxidation of 1 mM ferrocene in acetonitrile (0.1 M TEAP) at a scan rate of 50 mV/s. A two-electrode instrumental configuration with the Motorola D2 Kit and the Keithley 480 picoammeter was used for (a) and a three electrode format with the D2 Kit and the Metrohm VA Detector was employed for (b). The temperature was 22  $^{\circ}$ C.

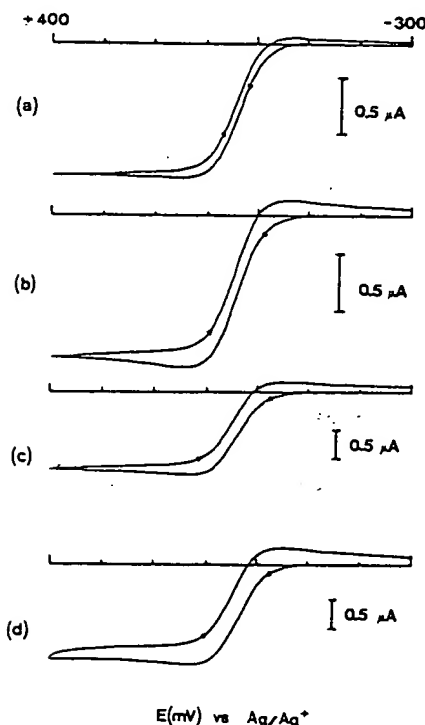


Figure 3. Cyclic voltammograms at 22  $^{\circ}$ C at a linear gold microelectrode of 1.18 cm length and about 0.6  $\mu$ m width for oxidation of 1 mM ferrocene in acetonitrile (0.1 M TEAP). The scan rates were 10 mV/s (a), 50 mV/s (b), 200 mV/s (c), and 1000 mV/s (d). The BAS 100 Electrochemical Analyzer was employed for these experiments.

steady-state experiment at a 2.5- $\mu$ m-radius gold microdisk electrode and was found to be  $37.4 \pm 2$  mV vs. Ag/Ag $^{+}$ .

Figure 2a shows a linear sweep voltammogram at a gold microdisk electrode with radius 2.5  $\mu$ m at a scan speed of 50 mV/s. This exhibits a steady-state response and is governed by the equation

$$E = E_{1/2}^{\circ} + RT/nF \ln ((i_d - i)/i) \quad (10)$$

where  $E$  is potential,  $E_{1/2}^{\circ}$  is the reversible half wave potential,  $i$  is the current, and  $i_d$  is the diffusion-controlled limiting current. Other symbols have the usual electrochemical meaning. Under conditions of cyclic voltammetry, complete overlap of forward and reverse scans occurs at slow scan rates when spherical diffusion is the predominant mode of mass transport to the electrode surface.

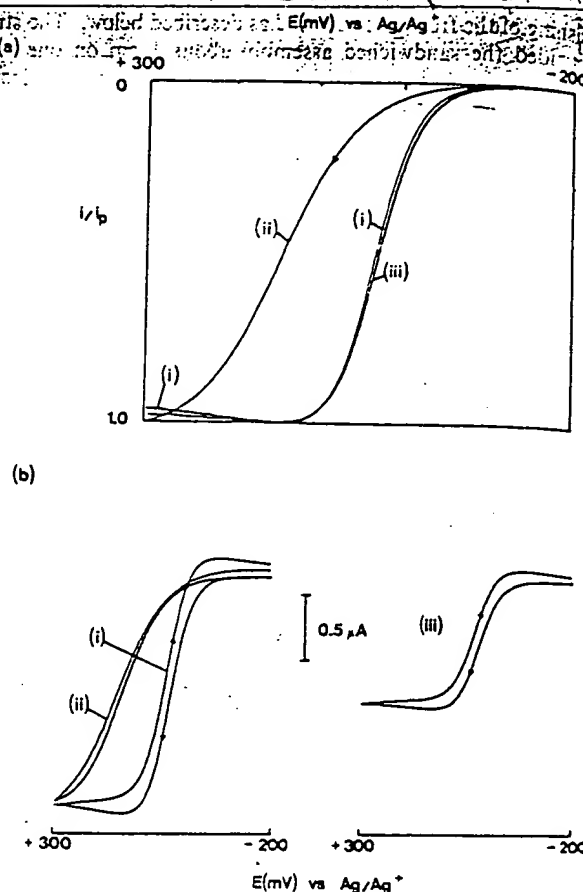


Figure 4. Comparison of computer simulated (i, ii) and experimental (iii) data for oxidation of 1 mM ferrocene in presence of a large excess (0.1 M TEAP) of supporting electrolyte at 22  $^{\circ}$ C. Both the normalized linear sweep data (a) and the cyclic voltammetric data (b) are depicted for an electrode length of 1.18 cm. The scan rate in all cases was 50 mV/s. (i) Simulation data for reversible case at an electrode width of 0.2  $\mu$ m. (ii) Simulation data for quasi-reversible case with  $k^0 = 0.09$  cm/s at an electrode width of 0.2  $\mu$ m. (iii) Experimental data for electrode width of about 0.6  $\mu$ m.

As linear diffusion becomes more pronounced, peak-shaped curves are observed as described theoretically<sup>18,20</sup> and experimentally.<sup>9</sup> In contrast, Figure 2b demonstrates that a linear electrode with a thickness considerably less than the diameter of the gold microdisk electrode produces a peak-shaped curve, which cannot be described by eq 10, nor does it have the appearance of a steady-state experiment. This is also reflected in the considerable dependence of the peak current on scan rate which is in contrast to the scan rate independence of the limiting current of microdisk electrodes. Figure 3 presents cyclic voltammograms of a linear electrode at different sweep rates. At all scan rates a peak is observed in either scan direction and a separation between forward and reverse sweeps is apparent. A microdisk electrode of radius 0.5  $\mu$ m does not show any of these characteristics for the same scan rates. Clearly a linear electrode produces large currents but its characteristics are not simply the summation of a linear combination of microdisk electrodes.

Over the scan rate range of 10–1000 mV/s for electrodes of thickness 0.4–0.8  $\mu$ m and length 1.18 cm good agreement with theory is observed with respect to shape, peak position, and dependence on the variables. Figure 4 depicts both computer simulation data and experimental data for linear sweep and cyclic voltammetric oxidation of 1 mM fc in presence of supporting electrolyte (0.1 M tetraethylammonium perchlorate, TEAP). Table II summarizes the simulated results for the forward scan at two sweep rates assuming full reversibility. The theory always predicts a nonsigmoidal response for both sweep directions; i.e., it is impossible to obtain a steady-state voltammogram under cylindrical diffusion conditions even if the radius or thickness of the microelectrode tends toward zero. This is consistent with the

TABLE II: Computer simulated results for ferrocene in presence of supporting electrolyte assuming full reversibility

width of linear electrode, $\mu$ m	cc microelectrode, $\mu$ m
0.2	0.
0.5	0.
2.0	0.
5.0	0.
10.0	1.
20.0	3.
40.0	6.
100.0	15.
0.2	0.
2.0	0.
100.0	15.

\* Conditions as in Table I.

findings of Aoki et al. that spherical diffusion separation between electrodes is consistent with findings.

Published value in the order of 0.1 cm with  $k^0 = 1000$  cm/s experimental data indicates a rate constant of 1000 cm/s. Wightman's findings of 50 mV/s the experimental data. Preliminary calculations of micrometer thick constants at conv progress to explicit of very fast electrode.

The absolute value is higher than those of Empirically, a half-cylinder appears closer to agreement between a half-cylinder diffusion of the electrode diffusional transport.

The theoretical appropriate for linear electrodes of 1  $\mu$ m. In the inverse show that the coefficient of 10 and 10. In the present case the linear electrode summarizes the electrodes develop desirable goal of could also be obtained < 0.1  $\mu$ m.

The peak current predicted by the electrodes with multiple linear electrodes are suitable length means implementation furthermore if these transient completely cylindrical

TABLE II: Computer Simulated Data for the Oxidation of 1 mM Ferrocene in Presence of a Large Excess of Supporting Electrolyte Assuming Full Reversibility<sup>a</sup>

width of linear electrode, $\mu\text{m}$	corresponding microcylinder radius, $\mu\text{m}$	scan rate, mV/s	total peak current, $\mu\text{A}$	peak current from planar diffusion only, $\mu\text{A}$	ratio planar/total peak current
0.2	0.0318	50	1.85	0.0068	0.00367
0.5	0.0796	50	2.20	0.017	0.00773
2.0	0.3183	50	2.77	0.068	0.0245
5.0	0.7958	50	3.28	0.17	0.0518
10.0	1.5915	50	3.83	0.34	0.089
20.0	3.1831	50	4.60	0.68	0.148
40.0	6.3662	50	5.74	1.16	0.202
100.0	15.9155	50	8.36	3.40	0.407
0.2	0.0318	1000	2.31	0.030	0.013
2.0	0.3183	1000	3.74	0.304	0.081
100.0	15.9155	1000	20.90	15.21	0.727

<sup>a</sup> Conditions as in Table I except that  $k^0 = 1000 \text{ cm/s}$  for simulations at a scan rate of 50 mV/s.

findings of Aoki et al.<sup>21</sup> and is in contrast to configurations in which spherical diffusion is predominant. In all our simulations a clear separation between forward and reverse sweeps is predicted which is consistent with the experimental findings presented in Figure 1.

Published values of  $k^0$  for conventional platinum electrodes are of the order of 0.1 cm/s.<sup>33</sup> The comparison of simulation data with  $k^0 = 1000 \text{ cm/s}$  (reversible case),  $k^0 = 0.09 \text{ cm/s}$ , and the experimental data on linear gold microelectrodes (Figure 4a) indicates a rate constant considerably greater than this value as does Wightman's data<sup>17</sup> at microdisk electrodes. At the scan rate of 50 mV/s the simulation data for the reversible case and the experimental data are virtually identical within experimental error. Preliminary calculations show that linear electrodes with sub-micrometer thickness are ideally suited to measure fast rate constants at convenient (low) sweep rates. Work is currently in progress to explore the use of such electrodes for measurement of very fast electron-transfer rates.

The absolute current magnitudes predicted theoretically are higher than those monitored experimentally (see Figure 4b). Empirically, a half-cylinder model rather than a cylinder model appears closer to experimental reality and provides extremely good agreement between experimental and theoretical currents. Use of a half-cylinder model does not significantly change the prediction of the electrode properties which are governed by nonlinear diffusional transport.

The theoretical model based on cylindrical diffusion seems appropriate for linear microelectrodes. Previous studies on microcylinders employed lengths of wire with radii from 10 to 100  $\mu\text{m}$ . In the investigations of Aoki et al.<sup>21</sup> theoretical calculations show that the contribution from planar diffusion is 45% and 85% at  $a = 10$  and 100  $\mu\text{m}$ , respectively, for a sweep rate of 50 mV/s. In the present case the contribution is less than 1% for widths of the linear electrodes  $< 1 \mu\text{m}$  and therefore negligible. Table II summarizes the simulated results for various conditions. For our electrodes developed in this work we have essentially achieved the desirable goal of pure cylindrical diffusion. Comparable conditions could also be obtained with microcylinder electrodes having radii  $< 0.1 \mu\text{m}$ .

The peak current is a linear function of electrode length as predicted by the theory. Furthermore, currents of parallel linear electrodes with the investigated spacing  $> 24 \mu\text{m}$  as well as of multiple linear electrodes connected in parallel which are typically 1 cm apart are additive at the  $\pm 4\%$  level. If the linear microelectrodes are sufficiently long their additive nature with respect to length means that currents become sufficiently large for simple implementation of transient electrochemical techniques. Furthermore if their widths are very thin we should be able to apply these transient techniques under conditions where diffusion is completely cylindrical. This situation is realized with the present

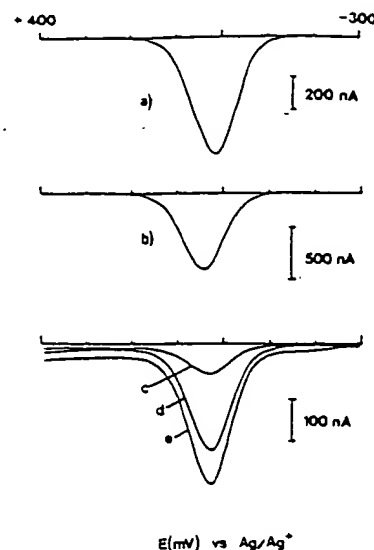


Figure 5. Differential pulse (a) and square wave (b-e) voltammograms at linear gold microelectrodes for oxidation of 1 mM ferrocene at 22 °C in acetonitrile with 0.1 M TEAP. The responses of a 1.18-cm-long linear electrode (a, b) and of two parallel, 0.31-cm-long lines (c, d) as well as their summation signal (e) are shown. The amplitudes and pulse widths were 50 mV and 60 ms for differential pulse (a) and 25 mV and 33.3 ms for square wave (b-e) voltammetry, respectively. The scan rates were 4 mV/s (a) and 60 mV/s (b-e) and the staircase ramp in all cases was 4 mV. The BAS 100 Electrochemical Analyzer was used for these experiments.

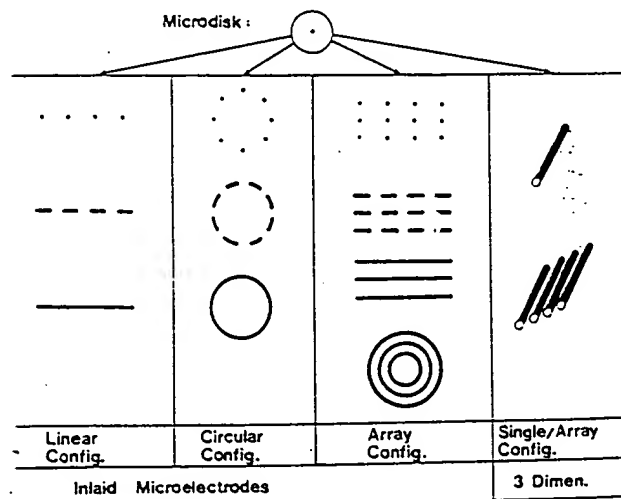


Figure 6. Configurations of inlaid microelectrodes (two-dimensional microelectrodes) and of microcylinder electrodes (three-dimensional microelectrodes).

electrodes. As shown in Figure 5a,b, extremely well-defined square wave and differential pulse curves may be obtained with commercially available instrumentation. In these results the square wave response gives a peak potential very close to  $E_{1/2}$  and the differential pulse peak potential is shifted to more positive potentials by  $\Delta E/2$  where  $\Delta E$  is the pulse amplitude.

The additive nature of the currents at linear electrodes is clearly revealed in the square wave voltammograms depicted in Figures 5c-e. That is, currents are essentially additive by either physically increasing their length or by electrochemical coupling in parallel of physically separated linear electrodes of the same or different widths. The relationship between microdisk electrodes, linear electrodes, and a ring electrode can now be understood. A schematic presentation of some of the different classes of microelectrodes is given in Figure 6. Provided (i) the electrodes have a sufficiently small radius or thickness so that linear diffusion is absent and (ii) individual sensing elements are sufficiently far apart, then the two extremes of a single-point electrode to a ring electrode represents a transformation from purely spherical diffusion to purely cylindrical diffusion.

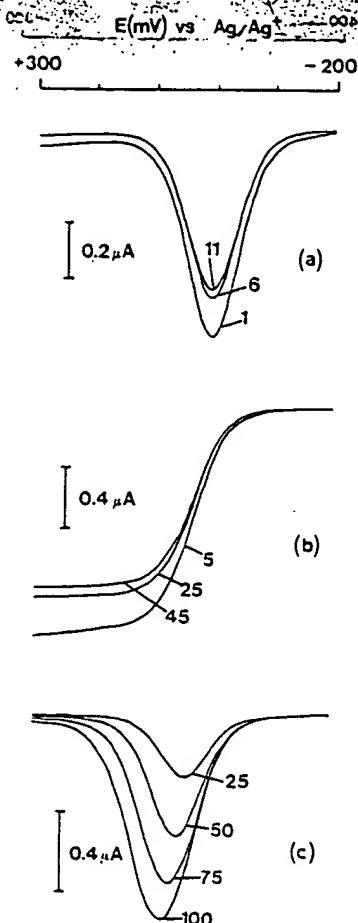


Figure 7. Multi-time-domain fast sweep differential pulse (a) and normal pulse responses (b) at a linear gold microelectrode of 1.18 cm length and about 0.6  $\mu\text{m}$  width for the oxidation of 1 mM ferrocene in 0.1 M TEAP at 22  $^{\circ}\text{C}$ . The variable amplitude pseudoderivative normal pulse data of experiment (b) is also depicted (c). The D2 Kit and the Metrohm potentiostat ( $i(t)$  output) were used. Differential and normal pulse widths as well as the amplitudes for the pseudoderivative normal pulse voltammograms are as indicated. The pulse amplitude in all cases was 50 mV and the scan rates were 113.6 mV/s (a) and 4.5 mV/s (b, c). The staircase ramp in all cases was 5 mV.

For a single microdisk electrode spherical diffusion leads to the observation of a steady-state response at conventional pulse widths. At short pulse widths planar diffusion terms lead to a time dependence in pulse voltammetry. For platinum microelectrodes of radius 0.3  $\mu\text{m}$  no time dependence is observed from 1 to 100 ms. As shown in Figure 7a,b a time-independent response is not observed at linear electrodes of submicrometer thickness. For pulse widths in the millisecond region the linear electrodes do not reach the steady-state response. They are clearly not operating under spherical diffusion laws (nor linear). The cylindrical diffusion model seems acceptable to describe such linear electrodes. The linear array electrodes reported in ref 12 exhibit intermediate time dependence under pulse conditions.

It has been well documented that microdisk electrodes under conditions of spherical diffusion are ideal for measurements in high-resistance solutions, e.g., in absence of deliberately added supporting electrolyte.<sup>11</sup> Linear electrodes operating under conditions of cylindrical diffusion also exhibit this characteristic (Figure 8) as would be expected.

With the electrodes of a thickness of about 0.1  $\mu\text{m}$  no peak current was observed in linear sweep experiments. The sigmoidal response obtained at these electrodes is very similar to that from the linear ensembles of inlaid microelectrodes<sup>13</sup> produced by the same materials. The polishing of the extremely thin lines without interrupting the continuous linear active electrode surface appears to be very difficult for the investigated electrodes with epoxy seal. This in turn suggests that these electrodes are better classified as linear arrays rather than linear microelectrodes. For thicknesses in the order of 0.4  $\mu\text{m}$  and larger linear sweep or cyclic voltam-

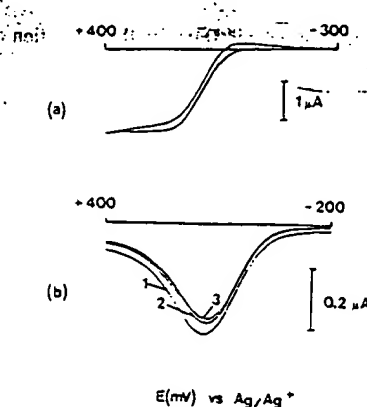


Figure 8. Voltammograms at linear microelectrodes for oxidation of 1 mM ferrocene without any deliberately added supporting electrolyte. The temperature was 22  $^{\circ}\text{C}$ . (a) Cyclic voltammogram at 50 mV/s with the BAS 100 using two parallel linear microelectrodes of 1.18 cm length. (b) Multi-time-domain fast sweep differential pulse voltammograms at a scan rate of 192.3 mV/s. Other experimental conditions as for Figure 7a.

mograms exhibiting a peak were monitored as shown in Figures 3 and 4. It is clear from the computer simulated data presented in this work that linear microelectrodes (and hence also very thin ring electrodes) will never yield a completely sigmoidal response in linear sweep or cyclic voltammetry. This is especially interesting in the case of very nearly 100% of cylindrical diffusion to the electrode surface which is in contrast to the microdisk electrode governed by spherical diffusion where genuinely steady state currents are observed. Recently O'Dea et al.<sup>34</sup> pointed out that square wave voltammetry exhibits a peak shape response whose shape might be invariant to electrode geometry, time scale of experiment, and mechanism of mass transport for reversible electrode reactions. This is certainly true for microdisk electrodes,<sup>34,35</sup> microcylinder electrodes,<sup>34</sup> arrays of microelectrodes,<sup>13</sup> linear microelectrodes as shown in this work, and very thin ring (microring) electrodes.<sup>36</sup> It is also clear from our work on microelectrodes<sup>13,35,36</sup> that not only square wave voltammetry but a whole range of transient voltammetric techniques in both solutions with added supporting electrolyte and systems of high resistance (without deliberately added electrolyte) are highly suitable for quantitative analysis. The results show that the shape of the faradaic current voltammograms are insensitive to the curvature and boundaries of the diffusion field around the electrodes. This behavior was predicted many years ago by Smith and co-workers<sup>37,38</sup> and represents one of several practical advantages with microelectrodes since the geometry of extremely small microelectrodes is difficult to control and to reproduce. Furthermore, the peak potential of transient techniques such as square wave voltammetry and ac voltammetry coincides with the half-wave potential of the redox couple, whereas the peak potential in differential pulse voltammetry is shifted to more positive potentials by  $\Delta E/2$  where  $\Delta E$  is the pulse amplitude. The peak widths indicate the number of electrons exchanged and the peak height is a measure of concentration.

## Conclusions

Voltammetry at very thin linear electrodes (width < 1  $\mu\text{m}$ ) can be adequately described by a theory based on cylindrical diffusion. The response of this class of electrode is a subset of microelectrodes encompassing the microdisk to microring electrode categories. They are intrinsically easier to construct than arrays of microdisk

(34) O'Dea, J.; Wojciechowski, M.; Osteryoung, J.; Aoki, K. *Anal. Chem.* 1985, 57, 954.

(35) Bixler, J. W.; Bond, A. M.; Lay, P. A.; Thormann, W.; van den Bosch, P.; Fleischmann, M.; Pons, B. S. *Anal. Chem.*, submitted for publication.

(36) Thormann, W.; Bond, A. M. *J. Electroanal. Chem.*, submitted for publication.

(37) Smith, D. E. In *Electroanalytical Chemistry*; Bard, A. J., Ed.; Marcel Dekker: New York, 1966; Vol. 1, p 1.

(38) Bond, A. M.; O'Halloran, R. J.; Ruzic, I.; Smith, D. E. *Anal. Chem.* 1976, 48, 872.

electrodes or rings of these classes of electrodes applied with corrosion in high-resistance linear gold microelectrode materials or semiconductor simulation data for microelectrodes with an almost perfectly suited to rates. Compar

## Dissociation

## Introduction

The development of molecular level interaction in the microscale dissociation on pursued by the involve strong c the dissociation products to the behavior,<sup>13-19</sup> the most simple kin where the surface molecule and it initially crushed interaction w by the high en relative simple present time fo principles point of such dissociation were reported to MgO(001) and collision-induced and for related ions<sup>21-23</sup> and hi the experimental emerges as to t process, and h features. One i a rotational phen rotational centrifugal rep

Permanent address: 9001 Zvezda, Yu

electrodes or ring electrodes and have the desirable properties of these classes of electrodes; i.e., transient techniques can be readily applied with conventional instrumentation and studies undertaken in high-resistance media. This work reports the fabrication of linear gold microelectrodes by thin-film techniques. The construction principles described here are not restricted to gold; other electrode materials, such as a whole range of metals, graphite, or semiconductors, can also be used. The combination of computer simulation data and experimental data shows that linear microelectrodes with submicrometer thicknesses are characterized by an almost purely cylindrical diffusion field and that they are ideally suited to measure fast rate constants at convenient sweep rates. Comparable conditions are predicted for microcylinder

electrodes with radii  $< 0.1 \mu\text{m}$  which are difficult to obtain from a practical point of view.

**Acknowledgment.** We thank J. W. Bixler, T. Mann, and D. R. MacFarlane for stimulating discussions, P. van den Bosch for his skilful assistance in the construction of the linear electrodes, D. Luscombe for technical assistance, and F. Rothery (CSIRO Belmont, Victoria) for the scanning electrode microscope work. The generous donation of gold metalloorganics by S. Pons, University of Utah, contributed to the research described in this paper and is gratefully acknowledged. This work was supported financially by the Australian Research Grants Scheme.

Registry No. Au, 7440-57-5; TEAP, 2567-83-1; ferrocene, 102-54-5.

## Dissociation Dynamics of Mass-Asymmetric Molecules in Impact on Solid Surfaces

Z. Bačić<sup>†</sup> and R. B. Gerber\*

Department of Physical Chemistry and The Fritz Haber Research Center for Molecular Dynamics,  
The Hebrew University of Jerusalem, Jerusalem 91904, Israel (Received: September 25, 1985)

The dissociation of heteronuclear molecules, induced by high-energy collisions with chemically inert surfaces, is studied by classical trajectories. Results for IBr and ICl in collisions with an MgO surface are compared with previous calculations for  $\text{I}_2$ . New qualitative effects are found in the case of ICl due to the high mass asymmetry, shown in the energy dependence of the dissociation probability, and in the velocity and the angular distribution of the dissociation fragments. The new features (compared with  $\text{I}_2$ ) are interpreted in terms of two different possible pathways for dissociation, corresponding respectively to collisions where the light or the heavy atom strikes the surface first. The results provide considerable insight into the role of collider masses in the dynamics of dissociation upon impact on surfaces.

### 1. Introduction

The development of sophisticated experimental techniques, such as molecular beam scattering, has transformed the field of gas-solid interactions in recent years by providing detailed information at the microscopic level on the processes involved.<sup>1</sup> Molecular dissociation on surfaces is among the topics most intensively pursued by the beam scattering method.<sup>2-11</sup> Many such reactions involve strong chemical binding forces between the surface and the dissociation fragments, resulting typically in sticking of the products to the surface, and leading to complicated dynamical behavior,<sup>12-19</sup> the theoretical treatment of which is difficult. The most simple kind of dissociation processes are, however, those where the surface is chemically inert with regard to the incoming molecule and its fragments. In such cases the molecule is essentially crushed against the steeply repulsive potential wall of its interaction with the surface, bond cleavage thus being induced by the high energy of the collision. These processes, by their relative simplicity, may offer some of the best prospects at the present time for understanding surface reactions from a first-principles point of view. Recently, first molecular beam studies of such dissociation processes induced by collisions with surfaces were reported by Amirav and Kolodney<sup>20,21</sup> for  $\text{I}_2$  in impact on MgO(001) and sapphire. Corresponding theoretical studies of collision-induced dissociation were carried out for  $\text{I}_2/\text{MgO}(001)$  and for related systems, using both classical trajectory simulations<sup>21-23</sup> and high-energy impulsive collision models.<sup>24-26</sup> From the experimental and theoretical results, a detailed physical picture emerges as to the dynamical mechanism of the fragmentation process, and how the latter is reflected in various observable features. One interesting conclusion is that dissociation occurs via a rotational predissociation mechanism: Fragmentation occurs when rotational excitation upon impact on the surface yields a centrifugal repulsion between the atoms that is high enough to

overcome the binding.<sup>21,24</sup> Another conclusion is that after molecular impact on the surface, a "hard" collision takes place between the fragments before the latter separate. This step in the dissociation process leads to interesting pronounced features in both the angular and the velocity distribution of the products.<sup>22,23,25</sup>

- (1) For a recent review see: Barker, J. A.; Auerbach, D. J. *Surf. Sci. Rep.* 1984, 4, 1.
- (2) Balooch, M.; Cardillo, M. J.; Miller, R. D.; Stickney, R. E. *Surf. Sci.* 1974, 46, 358.
- (3) Becker, C. A.; Cowan, J. P.; Wharton, L.; Auerbach, D. J. *J. Chem. Phys.* 1977, 67, 3394.
- (4) Sibener, S. J.; Lee, Y. T. *Rarefied Gas Dynam.* 1979, 11, 1417.
- (5) Bernasek, S. L. *Adv. Chem. Phys.* 1980, 41, 477.
- (6) Ceyer, S. T.; Somorjai, G. A. *Annu. Rev. Phys. Chem.* 1977, 28, 477.
- (7) Salmeron, M.; Gale, R. J.; Somorjai, J. A. *J. Chem. Phys.* 1977, 67, 5324.
- (8) Baldwin, D. A.; Murray, P. I.; Rabalais, J. W. *Chem. Phys. Lett.* 1981, 77, 403.
- (9) Comsa, G.; David, R. *Surf. Sci.* 1982, 117, 77.
- (10) Brown, L. S.; Bernasek, S. L. *J. Chem. Phys.* 1985, 82, 2110.
- (11) Robota, H. J.; Vielhaber, W.; Lin, M. C.; Segner, J.; Ertl, G. *Surf. Sci.* 1985, 155, 101.
- (12) McCreery, J. H.; Wolken, Jr., G. J. *J. Chem. Phys.* 1976, 64, 2845.
- (13) Gelb, A.; Cardillo, H. J. *Surf. Sci.* 1978, 75, 199.
- (14) Tantardini, G. F.; Simonetta, M. *Surf. Sci.* 1981, 105, 597.
- (15) Elkowitz, A. B.; McCreery, J. H.; Wolken, G. J. *J. Chem. Phys.* 1976, 64, 423.
- (16) Diebold, A.; Wolken, G. *Surf. Sci.* 1979, 82, 245.
- (17) Tully, J. *Acc. Chem. Res.* 1981, 14, 188.
- (18) Ron, S.; Shima, Y.; Baer, M. *Chem. Phys. Lett.* 1985, 116, 443.
- (19) Lee, C.-Y.; DePristo, A. E., a preprint.
- (20) Kolodney, E.; Amirav, A. *J. Chem. Phys.* 1983, 79, 464.
- (21) Kolodney, E.; Amirav, A.; Elber, R.; Gerber, R. B. *Chem. Phys. Lett.* 1984, 111, 366.
- (22) Elber, R.; Gerber, R. B. *Chem. Phys. Lett.* 1983, 97, 4.
- (23) Elber, R.; Gerber, R. B. *J. Chem. Phys.* 1984, 88, 1571.
- (24) Gerber, R. B.; Elber, R. *Chem. Phys. Lett.* 1984, 107, 141.
- (25) Elber, R.; Gerber, R. B. *Chem. Phys.* 1985, 92, 363.
- (26) Elber, R.; Kouri, D. J.; Gerber, R. B. *Chem. Phys.*, in press.

<sup>†</sup> Permanent address: Institute of Physics of the University, P.O.B. 304, 41001 Zagreb, Yugoslavia.